Real-space observation of (111) facet formation on vicinal Si(111) surfaces

H. Hibino
NTT Basic Research Laboratories, 3-1, Morinosato-Wakamiya, Atsugi, Kanagawa 243-01, Japan

Y. Homma
NTT Interdisciplinary Research Laboratories, 3-9-11 Midori-cho, Musashino, Tokyo 180, Japan

T. Ogino
NTT Basic Research Laboratories, 3-1, Morinosato-Wakamiya, Atsugi, Kanagawa 243-01, Japan
(Received 11 July 1994)

We report real-space observations of nucleation of (111) facets with 7×7 structures on a vicinal Si(111) surface using ultrahigh-vacuum scanning electron microscopy. As reported previously by Phaneuf *et al.*, who used low-energy electron microscopy [Phys. Rev. Lett. **67**, 2986 (1991)], (111) facets grow in very anisotropic shapes and are much longer along steps than normal to steps. In addition, we show that (1) the facet width is dependent on the heating current direction and (2) the facets tend to nucleate adjacent to one another. The second result is explained by the fact that stepped regions near the facets are not uniformly inclined but undulated. The local inclination is directly observed using *ex situ* atomic force microscopy and is in good agreement with calculated results accounting for step-motion kinetics. Additionally, we link the disappearance of the (111) facets to As adsorption.

I. INTRODUCTION

Vicinal semiconductor surfaces are an increasingly popular subject of investigation, especially because vicinal surfaces have been used for basic studies of epitaxial growth[1] and as substrates for fabrication of fractional superlattices.[2] We expect uniform distribution of single-layer steps on vicinal surfaces. However, real surfaces' step arrangements vary depending on parameters such as temperature, misorientation angle, and misorientation direction. On vicinal Si(111) surfaces, the step arrangements drastically change during the phase transition from 1×1 to 7×7 structures. Above the phase-transition temperature (T_c), vicinal Si(111) surfaces are uniformly covered with single-layer steps (3.14-Å high). However, below T_c, the surfaces have step arrangements that depend on the misorientation direction. On the surfaces misoriented to $[11\bar{2}]$ or $[1\bar{1}0]$, the 1×1-to-7×7 phase transition induces separation into 7×7-reconstructed (111) facets (henceforth 7×7-(111) facets) and stepped regions.[3,4] On the other hand, the $[\bar{1}\bar{1}2]$-misoriented surfaces are covered with single- and triple-layer steps.[5,6] Moreover, when the reconstruction is changed by adsorption of other materials, the steps are sometimes rearranged.[7,8]

In order to understand the thermodynamics of the step arrangement, we must clarify the relationship between the step arrangement and the reconstruction. It is, therefore, necessary to observe the step rearrangement during the reconstructive phase transition in real space. The real surface morphology, however, is determined not only by thermodynamics but also by kinetics. It has been reported that dc currents used to anneal the sample resistively affect the step arrangement.[9–15] This is probably because the dc currents affect the kinetics of diffusing atoms. Real-space observation of the step rearrangement is also essential in investigating the kinetics of the step arrangement.

The 1×1-to-7×7 phase transition on the $[1\bar{1}0]$- and $[11\bar{2}]$-misoriented surfaces has already been studied using low-energy electron microscopy (LEEM).[16,17] Phaneuf *et al.* showed that stripelike 7×7-(111) facets appear below T_c; at a given temperature, the facet width no longer increases without limit but is saturated at a certain width, which is determined by elastic relaxation.[16] They also showed that there is a spinodal that divides the faceting kinetics into unstable and metastable regions.[17] Also, we and our co-workers have studied nucleation and growth of the 7×7-(111) facet using high-temperature scanning tunneling microscopy (HT-STM).[18–20] The higher spatial resolution revealed that the nucleation of the 7×7-(111) facet requires a critical width and that changes in the width are quantized, the unit being a 7×7 unit cell.

In this paper, we explain how nucleation of the 7×7-(111) facet can be observed *in situ* using ultrahigh-vacuum scanning electron microscopy (UHV-SEM). We focus on the nucleation of the 7×7-(111) facet observed when the surface is quenched just below the temperature at which the 7×7-(111) facets appear. (The spinodal decomposition at lower temperatures is beyond the scope of this work.) We will show that the facet width is dependent on the heating current direction and that the facets nucleate in groups. This grouping of facets is explained by the kinetics of the step arrangement. The actual surface morphology must be known in order to investigate the kinetics, but imaging methods such as LEEM, HT-STM with the constant height mode, and SEM offer no quantitative information about the real surface morphology. Therefore, the morphologies of quenched samples

are obtained using *ex situ* atomic force microscopy (AFM). The surface morphologies are compared with calculated results for a model including step-motion kinetics. Additionally, as another example of the step arrangement during the reconstructive phase transition, surface morphological changes caused by As adsorption are observed using UHV-SEM.

II. EXPERIMENTAL

A UHV-SEM (base pressure $\sim 1.5\times10^{-9}$ Torr) unit equipped with a field-emission gun was used to observe phase transitions on vicinal Si(111) surfaces. To enhance surface sensitivity by reducing the penetration depth of the primary electron, a 25-keV electron beam was incident on the surface at a glancing angle of 2°–3°. With this configuration, a reflection high-energy electron-diffraction (RHEED) pattern in a selected area was also observed. The spatial resolution of the SEM at normal incidence was ~ 10 nm. The image-shortening effect parallel to the incident electron beam caused by the small glancing angle was partially compensated by reducing the beam raster width in this direction relative to the perpendicular direction. The vertical scale of SEM images in this paper is thus $\sim\frac{1}{5}$ of the horizontal scale. Additionally, in order to obtain real surface morphologies, AFM images were taken *ex situ* after the samples were removed from the vacuum.

Vicinal Si(111) wafers (*B*-doped, 1–10 Ω cm) were misoriented 2°, 4°, 6°, and 10° to $[11\bar{2}]$ and 5.6° to $[1\bar{1}0]$. Samples were cut into $0.3\times5\times15$-mm blocks. The long edge was parallel to the direction of the misorientation. The sample was chemically oxidized in a H_2SO_4:H_2O_2 (4:1) solution and then introduced into the SEM chamber through a load lock. The sample was degassed at about 550 °C for several hours and cleaned by flashing at 1250 °C. During observations, the longest edge was perpendicular to the electron beam. The sample was heated by passing dc currents through it. The current direction was either step up or step down. Arsenic was deposited using a Knudsen cell evaporator.

The sample temperature was measured using an infrared pyrometer. The 7×7-(111) facets appeared on 2°-, 6°-, and 10°-misoriented surfaces during cooling at approximately 867 °C, 825 °C, and 760 °C, respectively. However, in reality, the surface temperatures were not uniform on the sample. The temperature measured by the infrared pyrometer was not always the same as the temperatures in each local region observed in SEM images. Moreover, the temperature at which the 7×7-(111) facets appear during cooling is lower than the one at which they disappear during annealing.[18,20] Therefore, in this paper, we distinguish these temperatures as T_a and T_d, respectively, and surface temperatures are described in terms of the difference from T_a.

III. RESULTS AND DISCUSSION

A. Heating current direction dependence

Figure 1 shows UHV-SEM images of a vicinal Si(111) surface misoriented to $[11\bar{2}]$. The sample was quenched after being held for 1 min at T_a-1 K (824 °C). The heating current was step up in sample 1(a) and step down in 1(b). Here, white lines are 7×7-(111) facets, which appear with very high contrast using UHV-SEM. This contrast is due to the difference in local inclination[21] and the higher secondary electron yield from the 7×7 region than from the 1×1 region.[22] The region where the misorientation was smaller than the nominal misorientation looked bright, and vice versa. Dark regions around 7×7-(111) facets, which are quite pronounced in Fig. 1(a), have an inclination greater than the nominal misorientation.

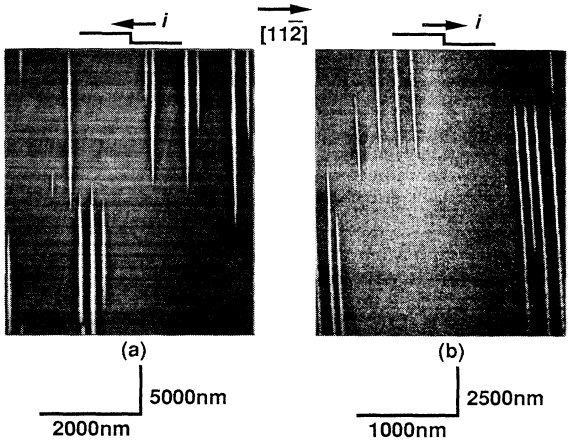

FIG. 1. UHV-SEM images of vicinal Si(111) surface misoriented 6° to $[11\bar{2}]$ taken at room temperature. The samples were quenched after annealing at T_a-1 K for 1 min by (a) step-up and (b) step-down currents.

As has been reported for LEEM,[16,17] the 7×7-(111) facets grew in a very anisotropic shape. The 7×7-(111) facet is much longer along steps than normal to steps. Comparing the two images in Fig. 1 reveals that the width of the 7×7-(111) facet depends on the heating current direction. With step-up current, the width is about 50 nm, but only about 20 nm with step-down current. When the sample misoriented 4° to $[11\bar{2}]$ was annealed by ac current, the facet width fell between the widths for the step-up and step-down currents. Therefore, the step-up current widens the facet width, and the step-down current narrows it. Moreover, because there was no difference in T_a, this current effect emerges with the appearance of the 7×7 reconstruction.

LEEM studies have proven the saturation of the 7×7-(111) facet width.[16] We also observed that this facet width saturated under step-down current. However, the width continuously increases under step-up current if the facet spacing is sufficient.[23] Figure 2 shows an example of the facet width growth on a vicinal Si(111) surface misoriented 5.6° to $[1\bar{1}0]$. The growth velocity normal to steps was much smaller than that parallel to steps. On the 6° misoriented to $[11\bar{2}]$ surface, for example, while the growth velocities parallel to the step (long side) were 80–110 nm/s for both current directions, the growth velocity normal to the step, which was estimated from the facet widths at annealing times of 1 and 5 min, was 0.3

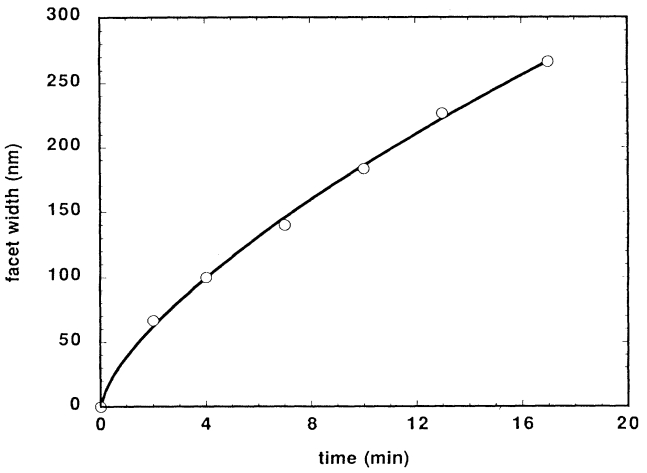

FIG. 2. Facet widening on a vicinal Si(111) surface misoriented 5.6° to $[1\bar{1}0]$, for a sample annealed at T_a-1 K (822 °C) by step-up current. The facet width of a certain facet was measured from SEM images taken during annealing. The solid curve is a guide for eye.

nm/s. The velocities parallel to the step were quite similar to the reported value for the 4°-misoriented surface to $[11\bar{2}]$.[7] Growth along the steps continued until another facet growing in the opposite direction approached within a certain distance.[16] In the nucleation, groups of facets were usually formed as shown in Fig. 1. The reason for this group formation will be explained later. When the surface was kept below T_a, nucleation and growth of the 7×7-(111) facets resulted in the surface being fully covered with them.

When the surface was further cooled, the facet width increase caused an increase in the inclination angle of the stepped region. Eventually, below 700 °C, contrasts appeared in the SEM images of the stepped regions. RHEED patterns from the surface included diffraction spots from a 12×1 reconstruction on the (331) facet.[19,24] These results show that (331) facets are formed in the stepped region. Our previous HT-STM results have shown that narrow (111) facets are made at the same time that the (331) facets are formed.[18,19] Therefore, the contrasts that appeared in the stepped regions are ascribed to the decomposition of the stepped region into the (331) and narrow (111) facets.

Next, we investigate the misorientation angle θ dependence of the 7×7-(111) facet nucleation. Figure 3 shows SEM images of vicinal Si(111) surfaces misoriented 2° [3(a) and 3(b)] and 10° [3(c) and 3(d)] to $[11\bar{2}]$. These surfaces, except that in Fig. 3(b), were also quenched after being held for 1 min at T_a-1 K (2°-misoriented surface; 866 °C, 10°-misoriented surface; 759 °C). For the 2°-misoriented surface annealed with step-down current, after being held for 1 min at T_a-1 K, 7×7-(111) facets nucleated all over the surface. Therefore, to investigate the initial stage of the facet formation, the surface shown in Fig. 3(b) was quenched after being held for 1–2 s at T_a-1 K. However, because the facet width saturates under step-down current and the facet width on the surface held for 20 s at T_a-1 K is equal to the facet width seen in Fig. 3(b), the facet width in Fig. 3(b) should have already reached its maximum. These images show that the facet width is dependent on the current direction at all misorientation angles, and the smaller θ, the larger the facet width.

The θ dependence of the facet width is shown in Fig. 4. In Ref. 16, because the samples were annealed by electron-beam bombardment, heating-current-induced effects could be neglected. On this sample, the 7×7-(111) facet has a saturation width, which is about 70 nm on the 4°-misoriented surface.[16] This value is close to that for the case of annealing with step-up current. However, with the step-up current, an isolated facet grew continuously during our experimental time (17 min). The facet width is, thus, dependent on the annealing time. Therefore, the coincidence between the value reported by Phaneuf *et al.* and our value is accidental and is probably due to the difference in the temperature to which the surface was quenched (in Ref. 16, the surface was cooled to T_a-3 K). On the other hand, we have already measured the 7×7-(111) facet width on the 10°-misoriented surface annealed by the step-down current using HT-STM. In HT-STM images just below T_a, the facet grows from a width of four 7×7 unit cells (92 Å) to six 7×7 unit cells (138 Å).[19] This value is in good agreement with the mea-

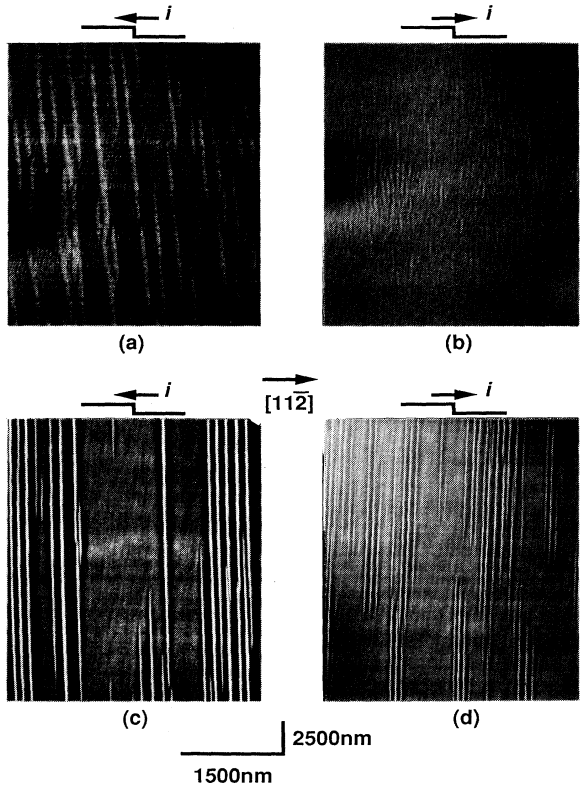

FIG. 3. UHV-SEM images of vicinal Si(111) surface misoriented 2° [(a) and (b)] and 10° [(c) and (d)] to $[11\bar{2}]$ taken at room temperature. The samples were quenched after being held at T_a-1 K for (b) 1–2 s and (a), (c), (d) 1 min.

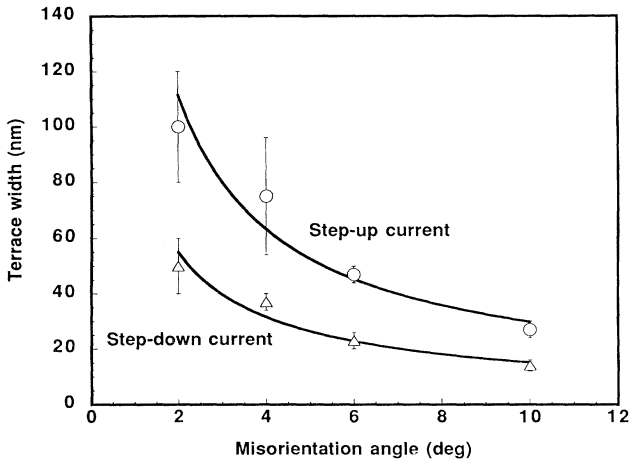

FIG. 4. Misorientation angle dependence of the 7×7-(111) facet width. The data are the average facet widths measured on lines drawn on SEM images along [11$\bar{2}$]. The samples except for the 2°-misoriented surface annealed by step-down current were quenched after being held for 1 min at T_a-1 K. The 2°-misoriented surface annealed by step-down current was quenched after being held for 1–2 s at T_a-1 K.

surements obtained using UHV-SEM.

Hysteresis loops in the temperature dependences of low-energy electron-diffraction spot intensities at the 1×1-to-7×7 phase transition have been reported.[4] We have also reported the temperature difference at the appearance and disappearance of 7×7-(111) facets using HT-STM.[18,20] Hysteresis was also confirmed using UHV-SEM. Since the difference between T_a and T_d was found to be dependent on the heating cycle, we only show a typical case. Figure 5 shows SEM images of a 6°-misoriented surface annealed using step-up current. After the surface was held for 5 min at T_a-1 K, the sample temperature was gradually increased. Image 5(a) was taken before the sample temperature increase; 5(b) and 5(c) were taken, respectively, after holding the sample for 30 s at T_a+20 K, and after additional annealing for 30 s at T_a+30 K. As the temperature increases, the facet narrows. The 7×7-(111) facet mainly grows by extension along steps. However, it did not shrink in a reverse-growth pattern. A decrease in width as well as shortening along the steps was noticeable. The difference between T_a and T_d was also dependent on the heating-current direction. When, after being held for 2 min at T_a-1 K, the sample temperatures were increased by 2-K increments with a 30-s hold following each increase, the differences between T_a and T_d for the step-up and the step-down currents on the 6° surface were about 42 and 16 K, respectively.

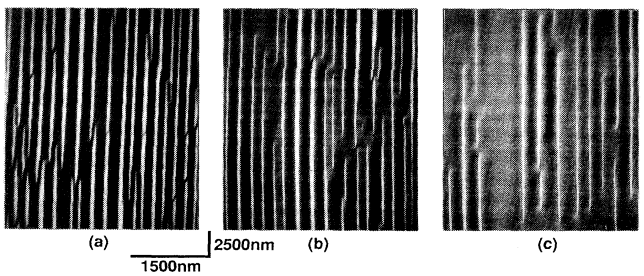

FIG. 5. UHV-SEM images of vicinal Si(111) surface misoriented 6° to [11$\bar{2}$]. The sample in panel (a) was quenched after annealing at T_a-1 K for 5 min. Then, it was sequentially annealed to the target temperatures and quenched. The samples in panels (b) and (c) were quenched after the temperature was raised to T_a+20 K and T_a+30 K, respectively. All the SEM images were taken at room temperature.

The effects of heating-current direction on the step arrangements on flat and vicinal Si(111) surfaces have been reported by many groups.[9–15] On a vicinal Si(111) surface, the effects are classified in four temperature regions: 1300 °C ≥ T ≥ 1200 °C, 1150 °C ≥ T ≥ 1050 °C, 950 °C ≥ T ≥ T_c, and $T \le T_c$.[14] In the highest temperature region (1300 °C ≥ T ≥ 1200 °C), the step-down current induces step bunching; however, the step-up current favors uniform step distribution. The current direction which induces step bunching is reversed between neighboring temperature regimes. Thus, in the lowest temperature region ($T \le T_c$), the step-up current induces step bunching. In this experiment, the 7×7-(111) facet grows continuously under step-up current. On the other hand, the step-down current keeps the facet narrower. The step-up current gives a wider facet than the step-down current. As described previously, groups of facets are formed in the initial stage of facet formation. The distance between facets in the same group is longer for step-up than for step-down current. Therefore, more steps are bunched under step-up current, which is consistent with previously reported results.[14]

B. As deposition

Because the step arrangement is closely related to the reconstruction on the terrace, adsorption of other materials may induce changes in the step arrangement.[7,8] For example, As adsorption under equilibrium conditions causes regular double-layer step arrays on vicinal Si(111) surfaces, regardless of the misorientation direction.[8] Figure 6 shows the morphological change during As adsorption. Images were taken 6(a) before adsorption, 6(b) after As was adsorbed for 20 s, 6(c) for 70 s, and 6(d) for 110 s, but not at the same position. This figure clearly indicates disappearance of the (111) facet due to As adsorption. This result is in good agreement with previously reported step rearrangement during As adsorption.[8]

C. Surface morphology

We obtained real surface morphologies at the initial stage of the 7×7-(111) facet formation using AFM. Although UHV-SEM images include information about the local inclination, this is not quantitative. Therefore, after the sample was quenched at the initial stage of the 7×7-(111) facet formation, it was taken out of vacuum, and the surface morphology was measured using AFM in air.

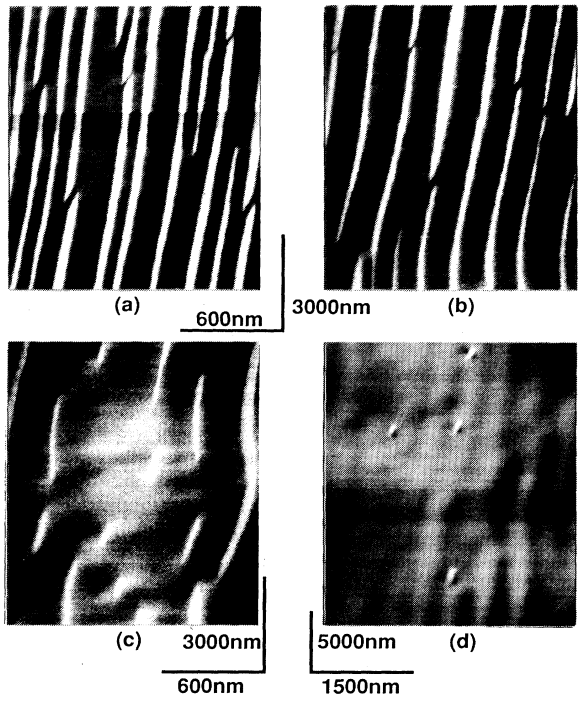

FIG. 6. UHV-SEM images of vicinal Si(111) surface misoriented 6° to [11$\bar{2}$] held at T_a-1 K (a) before As deposition, and (b)–(d) after being exposed to an As flux for 20 s, 70 s, and 110 s, respectively. The As flux corresponded to the partial pressure of $\sim 1\times 10^{-8}$ Torr. SEM images were taken at T_a-1 K with interruption of As flux. Facet width increased during interruption of As flux.

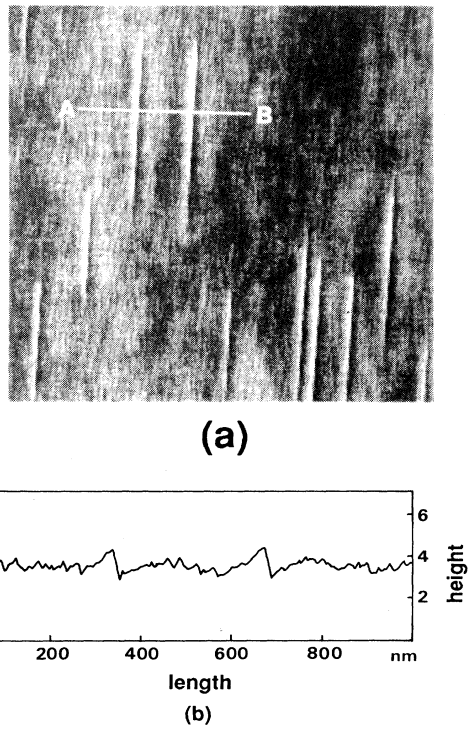

FIG. 7. (a) An AFM image of the vicinal Si(111) surface misoriented 10° to [11$\bar{2}$]. The sample was quenched from just below T_a. The AFM image was acquired in air after removing the sample from vacuum. The surface was, therefore, oxidized. The scanning area was 2500×2500 nm. (b) Cross section between A and B in (a).

Our AFM equipment is very sensitive to surface morphologies and can detect even a single-layer step.[25] The procedure has problems detecting changes in the surface morphologies during quench and oxidation. However, the cooling rate in this experiment was very fast (above 50 K/s), and changes in surface morphologies on highly misoriented surfaces are especially resistant to change because nucleation and growth of the 7×7-(111) facet require more mass transfer. On the other hand, Ross, Gibson, and Twesten reported using a UHV transmission electron microscope that interface steps are at the same positions as the steps on the original surface after oxidation[26] and Suzuki *et al.* reported that the crystallographic directions of the single-layer steps can be identified by AFM in air.[25] Thus, overall features can be regarded as unchanged.

Figure 7 shows an AFM image of a vicinal Si(111) surface misoriented 10° to [11$\bar{2}$]. Dispersed nucleation of 7×7-(111) facets can be clearly seen. Rough features on the stepped region are due to nucleation of the 7×7-(111) facet during quench. A cross section between A and B is shown in Fig. 7(b). This figure clearly shows that the stepped region has a curved shape. Regions immediately adjacent to the facet are inclined the most. This local inclination gradually decreases with increasing distance from the facet, and the local inclination becomes smaller than the nominal misorientation at a certain place. Afterwards, the local inclination approaches the nominal misorientation. This step distribution cannot be understood unless diffusion of atoms is taken into consideration. If diffusion were infinitely fast, an equilibrium step density would be reached instantaneously. Then the stepped region would be uniformly inclined and steps would be equally spaced. The shape of the stepped region reflects the kinetics of the step motion.

Grouping of 7×7-(111) facet nucleation in SEM images can be explained by the step distribution described above. T_c is dependent on the misorientation angle: The smaller the misorientation angle, the higher T_c. The step redistribution, therefore, causes T_c to be different from place to place. Because the regions immediately adjacent to the facet are inclined more than the nominal misorientation, their local T_c's are lower. However, away from these regions, there are regions inclined less than the nominal misorientation, so T_c is higher there. Nucleation of the 7×7-(111) facet, therefore, occurs preferentially there. Thus, the 7×7-(111) facets nucleate adjacent to one another. In order to confirm this idea, we compared the distance between neighbor facets with calculated surface morphologies in the vicinity of an isolated facet. This comparison will be presented later.

D. Modeling

When the 1×1-to-7×7 phase transition occurs only on the central terrace in a step train (Fig. 8), the difference in

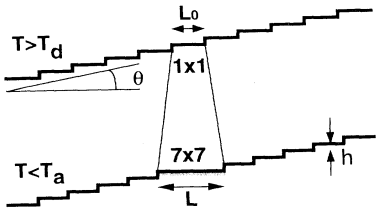

FIG. 8. Schematic views of step structures before and after the 1×1-to-7×7 phase transition. The 7×7-(111) facet appears at T_a during cooling, but the facet disappears at T_d ($\geq T_a$) during heating. L_0 is average terrace width determined by the misorientation angle θ. L is the 7×7-(111) facet width.

the total free energies per unit area before and after the transition is

$$\Delta F_{\text{total}} = 2\Delta E_{\text{edge}} - \Delta E_{\text{rec}} L + \Delta E_{\text{step}} + E_{el}(L) ,$$

where L is the width of the 7×7-(111) facet, ΔE_{edge} is the energy cost per unit length to make a 7×7-reconstructed step edge from a nonreconstructed one, ΔE_{rec} is the energy gain per unit area from forming the 7×7 reconstruction on the central terrace, ΔE_{step} is the change in the step interaction energy caused by the step redistribution, and E_{el} is the strain energy: $E_{el}(L) = -\gamma \ln(L/a)$, where γ is proportional to the square of the difference between surface stresses of the 7×7-(111) facet and nonreconstructed stepped region, and a is a length on the order of the 7×7 unit cell width.[16] As for the step interaction energy, the elastic and dipole-induced interactions are well known, and both are proportional to l^{-2}, where l is the distance between steps.[27,28] The free-energy cost due to restricting the step motion is proportional to $\langle l \rangle^{-2}$.[28,29] Therefore, we assume that the step interaction may be written as Gl^{-2}.

In order to reproduce the real surface morphology obtained using AFM, we modeled the 7×7-(111) facet formation, taking account of step-motion kinetics. In the following discussions, however, we ignore E_{el} for simplicity. We also ignore the effect of the heating current. The propriety of this omission will be discussed later. Because ΔE_{edge} is not dependent on L, it does not contribute to the step-motion kinetics. The step distribution is, therefore, determined by ΔE_{rec} and G, which we hereafter replace with $e = \Delta E_{\text{rec}} L_0$ and $g = G/L_0^2$, where L_0 is the nominal terrace width determined by the single-layer step height and the misorientation angle. Results of such modeling, following the assumption proposed by Nozières,[30] have already been shown in Fig. 2 in Ref. 16. This figure also shows local step density variation, and is consistent with our AFM results. However, the overall shape is expected to be dependent on e and g. Through our calculated results in Fig. 9, we can compare surface morphologies obtained when e is the same but g's are different. Recently Bartelt, Einstein, and Williams showed that the motion of steps calculated numerically using the theory proposed by Rettori and Villain[31] for the evolution of surface morphology is in good agreement with the Monte Carlo simulations of step motion.[32]

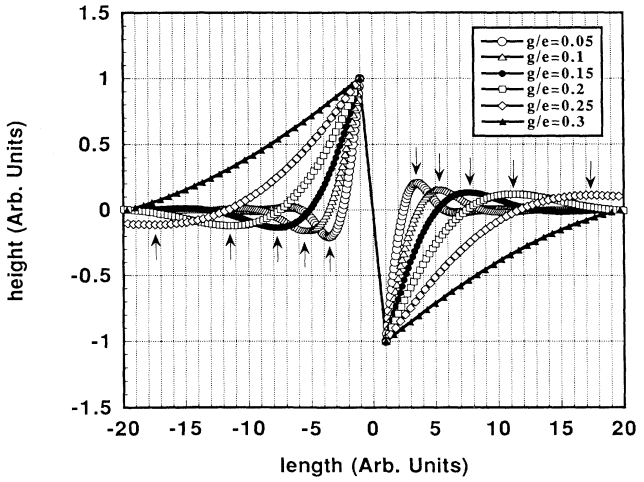

FIG. 9. Surface morphologies during an isolated facet growth. Surface morphologies are normalized by the facet width. They were the results of numerical integration of atom current density, which is calculated from the free energy of a vicinal surface using Rettori and Villain's theory (Ref. 31) for the evolution of surface morphology. e is the energy gain for forming the 7×7 reconstruction times, the nominal terrace width L_0 determined by the misorientation. g is the step interaction energy between steps L_0 apart. Surface morphologies obtained when e is the same but g's are different are shown. $g/e = 0.05$–0.3. $t = 100\,000\,00$ was selected so that the central facet width for $g/e = 0.15$ is about ten times larger than the width determined by the misorientation. The positions whose misorientations are equal to the nominal misorientation are indicated by arrows.

Therefore, we also used this theory for the step rearrangements during facet growth. Figure 9 shows that stronger step interaction causes smoother variation of step density. In this calculation, because the strain energy was neglected, the facet growth did not saturate. Kinetic theory predicts that if the facet growth is controlled by the surface diffusion of atoms, the facet width grows in time as $t^{1/4}$.[33] In our model, when the facet width growth is fitted to t^{α}, α is dependent on the growth time and g/e. The longer the growth time, the closer α is to $\frac{1}{4}$, and the larger g/e, the smaller α.

Since the surface morphology depends on g/e, comparison between the experimental results and the model calculations gives information about the relation between g and e. To fit the calculated and the AFM results, we compared the ratio R between the 7×7-reconstructed terrace width and the distance between the points where the inclination angle first equals the nominal misorientation angle away from the central terrace. R of the 10°-misoriented surface obtained from the AFM image in Fig. 7 is about 0.11. The model requires $g/e = 0.18$ for an R of 0.11. Using the reported value of G,[6,34,35] g for the 10°-misoriented surface is 1.4 meV/Å, so $g/e = 0.18$ gives $e = 7.8$ meV/Å. R of the 6°-misoriented surface was about 0.15. R of 0.15 corresponds to $g/e = 0.13$, resulting in $e = 3.7$ meV/Å.

The energy difference between "1×1" and 7×7 structures, $\Delta E_{\text{rec}}(T=0\text{ K})$, is estimated using the relation

$\Delta E_{rec}(T=0\ \text{K})=eT_c(\text{flat})/L_0[T_c(\text{flat})-T_c(\theta)]$. $\Delta E_{rec}(T=0\ \text{K})$'s estimated from the data of the 10°- and 6°-misoriented surfaces are 4.6 and 3.1 meV/Å^2. $\Delta E_{rec}(T=0\ \text{K})$ can also be estimated using calculated energies of reconstructed Si(111) surfaces. RHEED patterns from the Si(111) surface above T_c include diffusive $\sqrt{3}\times\sqrt{3}$ streaks,[36] which can be explained as effects of adatoms diffusing on the bulk-terminated 1×1 surface. Recent *ab initio* calculations show that the surface energy of the 7×7 reconstruction is lower by 60 meV/(1×1 cell) than for a 2×1 π-bonded chain model.[37,38] The energy of the $\sqrt{3}\times\sqrt{3}$ reconstruction is about 60 meV higher than in the π-bonded chain model.[39] However, a 2×2 structure, which is also explained by an adatom arrangement on the 1×1 surface, has an energy close to that of the 2×1 reconstruction. Therefore, $\Delta E_{rec}(T=0\ \text{K})$ is about 60 meV/(1×1 cell)=4.7 meV/Å^2. Furthermore, Williams *et al.* experimentally obtained the energy difference between "1×1" and 7×7 structures. $\Delta E_{rec}(T=T_c(\text{flat})-200\ \text{K})=0.8\pm0.3$ meV/Å^2 gives $\Delta E_{rec}(T=0\ \text{K})=4.5\pm1.7$ meV/Å.[35] These values are very close to our estimated $\Delta E_{rec}(T=0\ \text{K})$ for the 10°-misoriented surface, and $\Delta E_{rec}(T=0\ \text{K})$ for the 6°-misoriented surface is also in the error of the experimentally obtained $\Delta E_{rec}(T=0\ \text{K})$, which shows that our calculated surface morphologies are appropriate.

Next, in order to clarify that the surface morphology in the vicinity of an isolated facet consistently explains the facet nucleation in groups, we show the comparison between the neighbor facet distance and the calculated surface morphology. The surface in the vicinity of the facet undulates due to the kinetics of the step motion. The regions immediately adjacent to the facet are inclined more than the nominal misorientation. As the distance from the facet increases, the local inclination decreases, and there are regions inclined less than the nominal misorientation. 7×7-(111) facets are apt to nucleate there. Therefore, the distance between neighbor facets should be close to the distance between the facet and the region inclined less than the nominal misorientation. First, we obtain the ratio $R1$ of the facet width to the neighbor facet distance from the SEM images (Figs. 1 and 3). $R1$'s of the 10°-misoriented surfaces annealed by step-up and step-down currents are both about 0.19. $R1$'s of the 6°-misoriented surfaces annealed by step-up and step-down currents are 0.21 and 0.23. Next, we obtain the ratio $R2$ of the facet width to the distance between the facet and the region inclined least from the calculated surface morphologies. For the misorientation angle of 10°, $g/e=0.18$ well reproduced the surface morphology obtained by AFM. Then, $R2=0.17$ is obtained from the calculated surface morphology. For the misorientation angle of 6°, $g/e=0.13$, which gives $R2=0.23$. The good agreement between $R1$'s and $R2$'s indicates that the step arrangement during the 7×7-(111) facet nucleation causes the facet nucleation in groups.

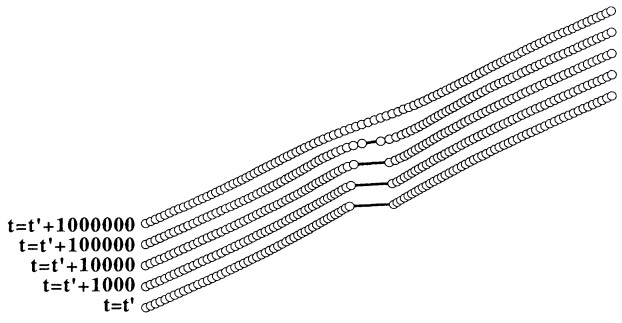

FIG. 10. Calculated step rearrangement during facet disappearance. The procedure of the calculation is the same as in Fig. 9. The facet width increases under the condition of $g/e=0.15$ till $t=t'$ ($=100\,000\,00$). Then, e was changed to 0.

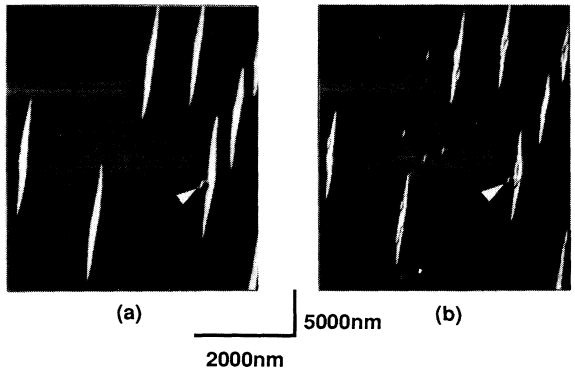

FIG. 11. UHV-SEM images of 6°-misoriented surface (a) quenched to room temperature after being held just below T_a for 5 min, and (b) then the same sample annealing to 900 °C, holding just below T_a for 1 min, and again quenching. The same location in (a) and (b) is marked by arrow heads.

Morphological change during the disappearance of the 7×7-(111) facet is also investigated using the model. Calculations assume that when the facet has grown wide enough, the energy gain due to the 7×7 reconstruction is lost. This corresponds either to the temperature increase up to T_c on a flat surface or to the reconstruction change from 7×7 to 1×1 by As adsorption. Figure 10 shows the calculated results. At $t=t'$, the energy gain of the central terrace is lost. Then, the region around the facet, whose inclination is greater than the nominal misorientation, rapidly changes, and the sharp edge between the (111) facet and the stepped region is lost; the (111) facet is smoothly connected to the stepped region. This is seen clearly in Figs. 5(b) and 5(c) and 6(b) and 6(c), where images show bright regions adjacent to the facets, and dark regions beyond. Figure 10 also shows that even after the facet has almost completely disappeared, the surface remains undulated, which is in good agreement with the experimental results [Fig. 6(d)]. Moreover, as shown in Fig. 10, because the shapes of the regions not close to the facet change slowly, smooth surface corrugation remains for a very long time. This is symbolically shown in Fig. 11. When the surface is kept just below T_a for 5 min, the nucleation of 7×7-(111) facets was observed [Fig. 11(a)]. Then [Fig. 11(b)], the surface was heated up to 900 °C, and again cooled to just below T_a. Comparison of the two images shows that new 7×7-(111) facets exist at the

same positions where such facets existed previously. This repeated nucleation at the same position is a result of the surface corrugation not completely vanishing even after 900 °C annealing.

Lastly, consider the propriety of ignoring the strain energy E_{el} and heating-current effect in our calculation. We estimated e/g by comparing the experimental (AFM) and calculated morphologies. Because the strain energy and the heating-current effect were ignored in the calculation, the estimated e/g includes uncertainty. We showed previously that $R1$'s obtained from SEM images are consistent with the calculated morphologies. $R1$'s obtained for the 10°- and 6°-misoriented surfaces hardly depend on the heating-current direction. $R1$ is affected very little by the heating-current direction, so the heating-current effect can, therefore, be safely ignored. This is because the step interaction determines the step distribution for a given facet width. Meanwhile, the strain energy E_{el} is a function of the facet width, so E_{el}, as well as the heating current, mainly change the facet width. Therefore, R would be barely changed by the inclusion of the strain energy in the calculation. However, when annealing is continued even after the facet width reaches its maximum value, the stepped region changes in shape. Indeed, the model shows that the gently curved region slowly changes in the shape during disappearance of the facet. Thus, R obtained experimentally would be little affected even when the facet width is saturated. The coincidence of $R1$'s estimated from the samples annealed by step-up and step-down currents also indicates that annealing after facet width saturation can be neglected in the case of quenching after holding for 1 min at $T_a - 1$ K.

IV. CONCLUSION

Nucleation of (111) facets with a 7×7 structure on a vicinal Si(111) surface was investigated using UHV-SEM. Results show that (1) the facet width depends on the heating-current direction and (2) the facets tend to nucleate adjacent to each other. The second result is caused by step redistribution with (111) terrace formation. The redistribution is well reproduced by a model that takes into account step-motion kinetics, and the model yields a valid rough estimate of the energy difference between 1×1 and 7×7 structures.

ACKNOWLEDGMENTS

We are grateful to M. Suzuki and Y. Kudo for AFM observation.

[1]J. H. Neave, P. J. Dobson, B. A. Joyce, and J. Zhang, Appl. Phys. Lett. **47**, 100 (1985).
[2]T. Fukui and H. Saito, J. Vac. Sci. Technol. B **8**, 1373 (1988).
[3]R. J. Phaneuf and E. D. Williams, Phys. Rev. Lett. **58**, 2563 (1987).
[4]R. J. Phaneuf, E. D. Williams, and N. C. Bartelt, Phys. Rev. B **38**, 1984 (1988).
[5]R. J. Phaneuf and E. D. Williams, Phys. Rev. B **41**, 1991 (1990).
[6]X.-S. Wang, J. L. Goldberg, N. C. Bartelt, T. L. Einstein, and E. D. Williams, Phys. Rev. Lett. **65**, 2430 (1990).
[7]F. Jentzsch and M. Henzler, Appl. Phys. A **46**, 119 (1988).
[8]T. R. Ohno and E. D. Williams, J. Vac. Sci. Technol. B **8**, 874 (1990).
[9]A. V. Latyshev, A. L. Aseev, A. B. Krasilnikov, and S. I. Stenin, Surf. Sci. **213**, 157 (1989).
[10]A. V. Latyshev, A. L. Aseev, A. B. Krasilnikov, and S. I. Stenin, Surf. Sci. **227**, 24 (1990).
[11]A. Yamanaka, H. Ohse, and K. Yagi, *Proceedings of the Twelfth International Congress for Electron Microscopy* (San Francisco Press, San Francisco, 1990), p. 306.
[12]H. Tokumoto, K. Miki, and K. Kajimura, J. Cryst. Growth **99**, 1392 (1990).
[13]H. Tokumoto, K. Miki, and Y. Morita, Ultramicroscopy **42-44**, 816 (1992).
[14]Y. Homma, R. J. McClelland, and H. Hibino, Jpn. J. Appl. Phys. **29**, L2254 (1990).
[15]Y. Homma, M. Suzuki, and H. Hibino, Appl. Surf. Sci. **60/61**, 479 (1992).
[16]R. J. Phaneuf, N. C. Bartelt, E. D. Williams, W. Swiech, and E. Bauer, Phys. Rev. Lett. **67**, 2986 (1991).
[17]R. J. Phaneuf, N. C. Bartelt, E. D. Williams, W. Swiech, and E. Bauer, Phys. Rev. Lett. **71**, 2284 (1993).
[18]M. Suzuki, Y. Homma, H. Hibino, T. Fukuda, T. Sato, M. Iwatsuki, K. Miki, and H. Tokumoto, J. Vac. Sci. Technol. A **11**, 1640 (1993).
[19]H. Hibino, T. Fukuda, M. Suzuki, Y. Homma, T. Sato, M. Iwatsuki, K. Miki, and H. Tokumoto, Phys. Rev. B **47**, 13 027 (1993).
[20]M. Suzuki, Y. Homma, H. Hibino, T. Fukuda, T. Sato, M. Iwatsuki, K. Miki, and H. Tokumoto, Jpn. J. Appl. Phys. **32**, 3247 (1993).
[21]Y. Ishikawa, N. Ikeda, M. Kenmochi, and T. Ichinokawa, Surf. Sci. **159**, 256 (1985).
[22]Y. Homma, M. Suzuki, and M. Tomita, Appl. Phys. Lett. **62**, 3276 (1993).
[23]In this experiment, annealing for about 20 min causes SiC particles to form on the surface. Therefore, 17 min was the longest annealing time that we confirmed for the continuous growth of the facet width.
[24]H. Hibino, Y. Kobayashi, Y. Shinoda, and K. Sugii, Jpn. J. Appl. Phys. **30**, 1337 (1991).
[25]M. Suzuki, Y. Kudoh, Y. Homma, and R. Kaneko, Appl. Phys. Lett. **58**, 2225 (1991).
[26]F. M. Ross, J. M. Gibson, and R. D. Twesten, Surf. Sci. **310**, 243 (1994).
[27]V. I. Marchenko and A. Ya Parshin, Zh. Eksp. Teor. Fiz. **79**, 257 (1980) [Sov. Phys. JETP **52**, 129 (1981)].
[28]C. Jayaprakash, C. Rottman, and W. F. Saam, Phys. Rev. B **30**, 6549 (1984).
[29]M. E. Fisher and D. S. Fisher, Phys. Rev. B **25**, 3192 (1982).
[30]P. Nozières, J. Phys. (Paris) **48**, 1605 (1987).
[31]A. Rettori and J. Villain, J. Phys. (Paris) **49**, 257 (1988).
[32]N. C. Bartelt, T. L. Einstein, and E. D. Williams, Surf. Sci.

312, 411 (1994).
[33]W. W. Mullins, J. Appl. Phys. **28**, 333 (1957).
[34]C. Alfonso, J. M. Bermond, J. C. Heyraud, and J. J. Metois, Surf. Sci. **262**, 371 (1992).
[35]E. D. Williams, R. J. Phaneuf, J. Wei, N. C. Bartelt, and T. L. Einstein, Surf. Sci. **294**, 219 (1993).
[36]S. Ino, Jpn. J. Appl. Phys. **16**, 891 (1977).
[37]I. Stich, M. C. Payne, R. D. King-Smith, J.-S. Lin, and L. C. Clarke, Phys. Rev. Lett. **68**, 1351 (1992).
[38]K. D. Brommer, M. Needels, B. E. Larson, and J. D. Joannopoulos, Phys. Rev. Lett. **68**, 1355 (1992).
[39]R. D. Meade and D. Vanderbilt, Phys. Rev. B **40**, 3905 (1989).

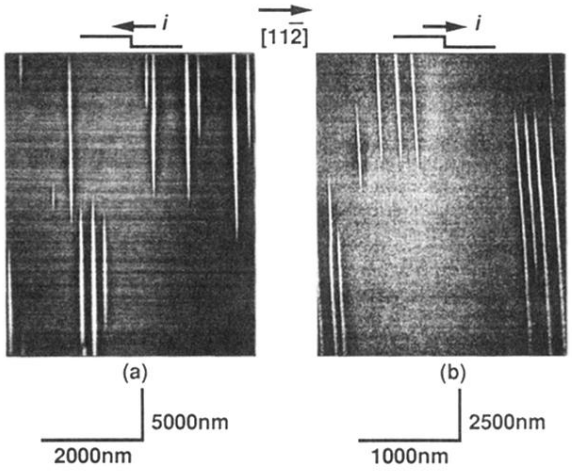

FIG. 1. UHV-SEM images of vicinal Si(111) surface misoriented 6° to [11$\bar{2}$] taken at room temperature. The samples were quenched after annealing at $T_a - 1$ K for 1 min by (a) step-up and (b) step-down currents.

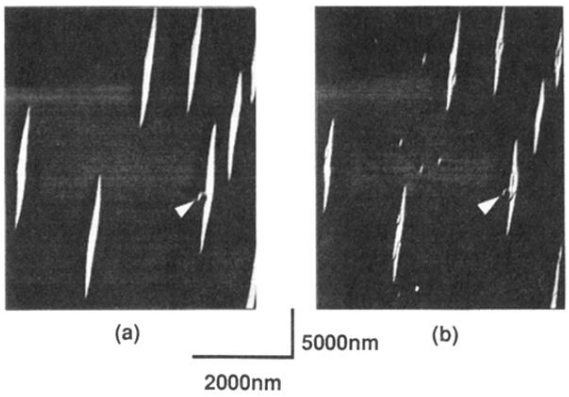

FIG. 11. UHV-SEM images of 6°-misoriented surface (a) quenched to room temperature after being held just below T_a for 5 min, and (b) then the same sample annealing to 900 °C, holding just below T_a for 1 min, and again quenching. The same location in (a) and (b) is marked by arrow heads.

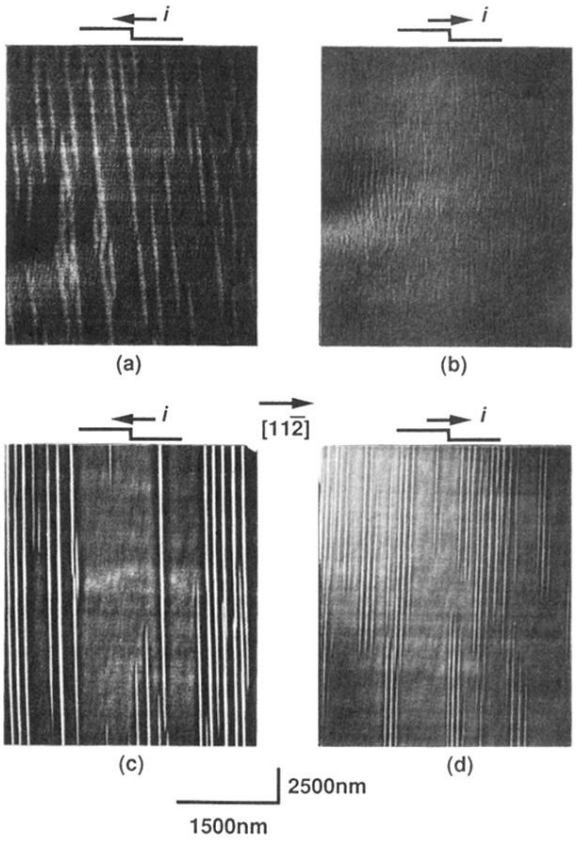

FIG. 3. UHV-SEM images of vicinal Si(111) surface misoriented 2° [(a) and (b)] and 10° [(c) and (d)] to [11$\bar{2}$] taken at room temperature. The samples were quenched after being held at $T_a - 1$ K for (b) 1–2 s and (a), (c), (d) 1 min.

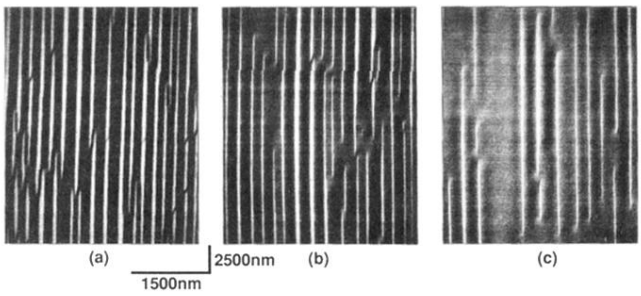

FIG. 5. UHV-SEM images of vicinal Si(111) surface misoriented 6° to $[11\bar{2}]$. The sample in panel (a) was quenched after annealing at $T_a - 1$ K for 5 min. Then, it was sequentially annealed to the target temperatures and quenched. The samples in panels (b) and (c) were quenched after the temperature was raised to $T_a + 20$ K and $T_a + 30$ K, respectively. All the SEM images were taken at room temperature.

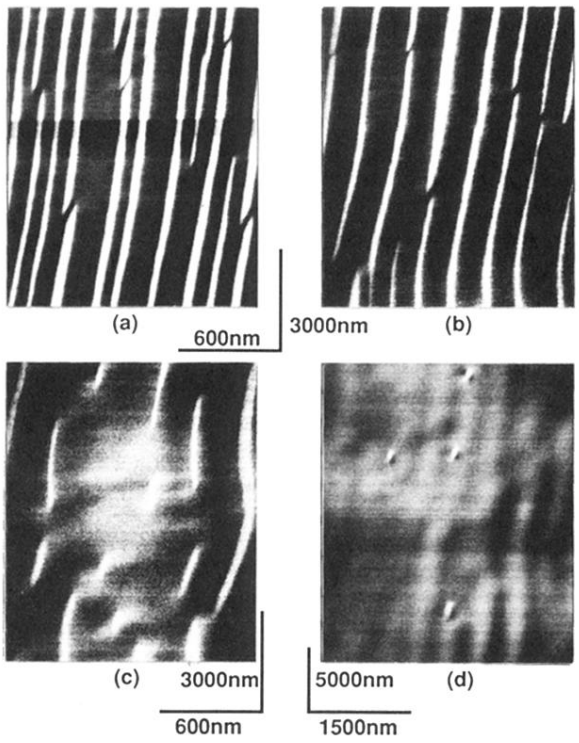

FIG. 6. UHV-SEM images of vicinal Si(111) surface misoriented 6° to $[11\bar{2}]$ held at $T_a - 1$ K (a) before As deposition, and (b)–(d) after being exposed to an As flux for 20 s, 70 s, and 110 s, respectively. The As flux corresponded to the partial pressure of $\sim 1 \times 10^{-8}$ Torr. SEM images were taken at $T_a - 1$ K with interruption of As flux. Facet width increased during interruption of As flux.

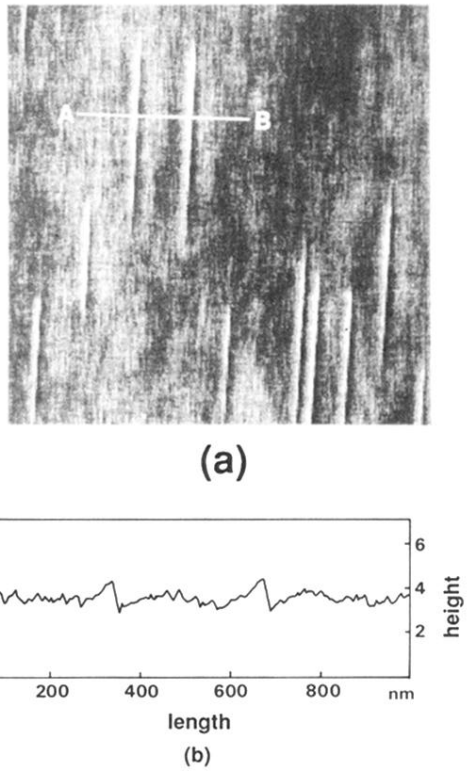

FIG. 7. (a) An AFM image of the vicinal Si(111) surface misoriented 10° to $[11\bar{2}]$. The sample was quenched from just below T_a. The AFM image was acquired in air after removing the sample from vacuum. The surface was, therefore, oxidized. The scanning area was 2500×2500 nm. (b) Cross section between A and B in (a).